Quantitative Ischemia Detection During Cardiac Magnetic Resonance Stress Testing by Use of FastHARP

Dara L. Kraitchman, VMD, PhD; Smita Sampath, MSE; Ernesto Castillo, MD; John A. Derbyshire, PhD; Raymond C. Boston, PhD; David A. Bluemke, MD, PhD; Bernhard L. Gerber, MD, PhD; Jerry L. Prince, PhD; Nael F. Osman, PhD

Background—Because ECG alterations caused by ischemia cannot be reliably detected in the high-field MRI environment, detection of wall motion abnormalities is often used to ensure patient safety during stress testing. However, an experienced observer is needed to detect these abnormalities. In this study, we investigate the use of fast harmonic phase (FastHARP) MRI for the quantitative, operator-independent detection of the onset of ischemia during acute coronary occlusion.

Methods and Results—Eight mongrel dogs underwent an acute 2-minute closed-chest coronary artery occlusion while continuous FastHARP images were acquired. Full regional wall strain was determined every other heartbeat in a single short-axis imaging slice. After 5 minutes of reperfusion, a second 2-minute ischemic episode was induced during the acquisition of conventional cine wall-motion images. The time at which ECG alterations were observed during the first ischemic period was recorded. The time from occlusion to the detection of ischemia, based on a consensus of 2 blinded observers, was determined for MRI. No significant ischemia was present in 2 animals. In the remaining animals, the onset of ischemia was detected significantly earlier by FastHARP than by cine MRI (9.5 ± 5 versus 33 ± 14 seconds, $P<0.01$). HARP ischemia detection preceded ECG changes, on average, by 54 seconds.

Conclusions—The rapid acquisition and detection of induced ischemia with FastHARP MRI shows promise as a nonsubjective method to diagnose significant coronary lesions during MR stress testing. **(*Circulation*. 2003;107:2025-2030.)**

Key Words: magnetic resonance imaging ■ myocardial contraction ■ coronary disease ■ systole ■ ischemia

The detection of myocardial ischemia on the basis of wall motion abnormalities (WMAs) during dobutamine stress echocardiography is well established.[1] The safety and success of dobutamine stress echocardiography for detecting coronary artery disease relies largely on the fact that the development of WMAs often precedes the development of ECG abnormalities or chest pain.[2] Recently, MRI has been suggested as an alternative method of detecting WMAs, with a diagnostic accuracy similar to that of dobutamine stress echocardiography. Moreover, MRI is especially well-suited to problematic patient populations, such as individuals with a large body habitus or poor echocardiographic windows.[3–5] However, the inability to obtain a diagnostic ECG in the MR environment has raised concerns about the safety of dobutamine stress testing.

Indeed, the detection of ECG repolarization abnormalities (eg, ST-segment alterations or T-wave morphology changes) is often not possible during MRI because of the magnetohydrodynamic effects, in which large-vessel blood flow in the high magnetic field creates extraneous voltages on the ECG.[6] Moreover, MRI stress wall-motion studies are typically not acquired continuously (ie, in real time), as with echocardiography, but rather during breath-held acquisitions. Therefore, WMAs can be determined only after some delay. However, perhaps the biggest problem with both dobutamine stress echocardiography and stress cine MR wall-motion studies is the variability in interpretation of the study.[7]

Tagged MRI[8,9] with strain quantification offers an alternative nonsubjective method of detecting regional WMA with greater accuracy than that of wall-thickening techniques.[10] However, tagged MR images are typically acquired over multiple breath-holds, with cumbersome manual postprocessing that necessitates offline analysis. Thus, this technique is not readily amenable to real-time detection of ischemia in the clinical setting. The harmonic phase (HARP) method[11,12] provides a simple solution for the rapid postprocessing of

Received October 28, 2002; revision received January 16, 2003; accepted January 16, 2003.

From Johns Hopkins University, School of Medicine, Departments of Radiology (D.L.K., E.C., D.A.B., N.F.O.) and Medicine, Division of Cardiology (B.L.G.), and Department of Electrical Engineering (S.S., J.L.P., N.F.O.), Baltimore, Md; National Institutes of Health, National Heart, Lung, and Blood Institute, Bethesda, Md (J.A.D.); and University of Pennsylvania, School of Veterinary Medicine, Kennett Square, Pa (R.C.B.).

Dr Kraitchman receives grant support from Berlex Laboratories, Inc. Drs Osman and Prince have equity interest in Diagnosoft, Inc.

Correspondence to Dara L. Kraitchman, Johns Hopkins University, Department of Radiology, MRI, 601 N Caroline St, No. 4231, Baltimore, MD 21287-0845. E-mail dara@mri.jhu.edu

Circulation **is available at http://www.circulationaha.org** **DOI: 10.1161/01.CIR.0000062684.47526.47**

tagged MR images. Therefore, the aim of this work was to develop a rapid, non–breath-hold method for imaging and detecting the onset of ischemia, as might occur during stress testing. By combining a rapid imaging scheme (FastHARP) with the rapid HARP postprocessing techniques, a color-coded overlay of regional strain can be displayed with ≈1 heartbeat delay to allow for rapid identification of strain abnormalities with minimal user training.

To validate the FastHARP technique, an animal model of acute ischemia during MRI was studied and compared with conventional cine MRI and ECG ischemic changes.

Methods

Animal Protocol

All animal studies were approved by our Institutional Animal Care and Use Committee and comply with the *Guide for the Care and Use of Laboratory Animals* (NIH Publication no. 80-23, revised 1985). Eight mongrel dogs (20 to 25 kg; Bruce Ritz Kennels, Shippensburg, PA) were preanesthetized with 10 mg/kg ketamine, 2.4 mg/kg xylazine, and 0.02 mg/kg atropine IM. The dogs were induced with 25 mg/kg thiopental IV, intubated, and mechanically ventilated with 1% to 2% isoflurane and 100% oxygen.

A right carotid artery cutdown was performed to place an 8F introducer sheath (Meditech, Boston Scientific). A 6F pigtail catheter (Cordis) was advanced via the carotid artery into the left ventricle for injection of radiolabeled microspheres to measure baseline regional myocardial blood flow. The pigtail catheter was then removed.

Before coronary catheterization, the dog was placed on a continuous infusion of lidocaine (2 mg $\cdot$ kg^{-1} $\cdot$ min^{-1} IV). The ECG and arterial blood pressure were monitored throughout the remainder of the study. From the carotid introducer, the left main coronary artery was engaged under x-ray fluoroscopy with an 8F right Judkins guiding catheter (Cordis). A 0.014-inch coronary guidewire was advanced into either the left anterior descending (LAD) or left circumflex (LCx) coronary artery. A deflated coronary angioplasty balloon (Cordis) was advanced over the guidewire into the proximal LAD or LCx. The guiding catheter was then removed from the left main coronary artery without disturbing the angioplasty balloon.

After balloon placement, the animal was transported to the adjacent MRI suite. Once at the MR scanner, the guidewire was removed from the coronary artery without disturbing the coronary balloon. Acute ischemia without infarction (based on triphenyltetrazolium chloride [TTC] staining) was induced by a 2-minute inflation of the angioplasty balloon while continuous MR images were acquired to monitor the onset of ischemia. The balloon was then deflated to allow for reperfusion for ≥5 minutes. The balloon was then reinflated for a second 2-minute coronary artery occlusion while MR imaging was performed. The balloon was then deflated.

ECG alterations indicative of ischemia were determined during the FastHARP MRI scan by observing the display of an optical MR-compatible ECG system (MedRad). These alterations consisted of either an increased amplitude of the T wave (ie, >25% of R wave) or a biphasic T wave that was not present before ischemia. Because of the magnetohydrodynamic effect and the use of a nonstandard electrode configuration on the chest, subtle ischemic changes, such as ST-segment depression, were not seen.

After imaging, the animal was returned to the x-ray suite, and the pigtail catheter was placed in the left ventricle via a femoral artery approach. The balloon angioplasty catheter was reinflated, and microspheres were injected into the left ventricle to determine the location and extent of the ischemic bed. After humane euthanasia, the chest was opened, balloon placement was confirmed, and the heart was excised and sliced along the short-axis planes for TTC staining and microsphere analysis.

MRI Protocol

All animals were imaged in a 1.5-T MR scanner (CV/i, General Electric) with a 4-channel, phased-array, transmit-receive coil placed over the heart. The animal was placed in the right decubitus position, and axial scout images were acquired to locate the left ventricle.

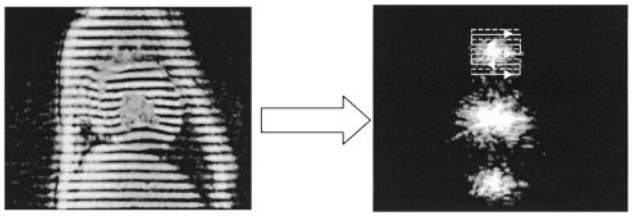

Figure 1. A 1-1 SPAMM-tagged MR image (left) consists of a set of distinct peaks in the Fourier domain (right). Inverse Fourier transform of a single off-center peak yields a phase image that contains motion information. FastHARP imaging significantly shortens imaging time by acquiring a limited portion of k-space (lines) around 1 spectral peak for each tag direction.

HARP imaging is based on the knowledge that spatial modulation of magnetization (SPAMM)–tagged MR images[8,13] have distinct spectral peaks in the Fourier domain. Each off-centered spectral peak contains motion information in a direction perpendicular to the tag lines. By taking the inverse Fourier transform of a single off-centered spectral peak, a complex image is formed, which has a phase that is linearly related to this directional component of the true motion. The material points that share the same harmonic phase in successive cardiac phases can be determined to track small motions.[11] Moreover, the gradient of the phase images from 2 orthogonal sets of SPAMM tag lines can be calculated to determine the 2D deformation or strain.[12]

The FastHARP imaging sequence exploits the concept that only 1 of the spectral peaks for each tag direction must be acquired for the calculation of myocardial strain. Thus, a limited portion of the k-space data centered around a single off-centered spectral peak can be acquired (Figure 1), thereby reducing image acquisition time without sacrificing information about myocardial motion and strain.

Ten to 15 cardiac frames or phases in a single short-axis slice were acquired every heartbeat by the fast gradient-echo echo planar imaging hybrid FastHARP pulse sequence with 1-1 SPAMM[8] tag directions alternating between 0 and 90° tags every heartbeat. For each cardiac frame, the desired harmonic peak from the tagging pulse sequence was acquired as a 32×32 matrix with the following image parameters: 62.5-kHz bandwidth (BW); 28-cm field of view (FOV); 11.3 ms repetition time (TR); 3.3 ms echo time (TE); echo train length (ETL) 8; 32 views per segment (vps); 0.875-mm tag spacing; 10-mm slice thickness; and flip angle=15°. Thus, temporal resolution of each FastHARP image was ≈45 ms. Images acquired from 2 successive heartbeats are sufficient to compute 2D strain measures. MRI k-space data were synchronously transferred to an external Sun workstation for reconstruction and display of synthetic tagged images.

In all studies, FastHARP images were acquired continuously for ≈20 to 30 seconds before balloon inflation until 1 to 2 minutes after the inflation of the balloon, at which point the balloon was deflated. After a ≥5-minute reperfusion interval, cine MRIs were acquired on the same short-axis slice during a 2-minute balloon inflation.

For the first 2 animals, cine MR images were acquired using the standard cine monitoring mode, a non–ECG-gated fast gradient echo pulse sequence with an echo-train readout. The imaging parameters were 125-kHz BW; ETL 8; 11.2 ms TR; 1.2 ms TE; 128×128 matrix; and 64 vps. Because of image buffer limitations, only ≈30 seconds of images could be acquired at a shot, followed by small pauses to restart the scan. Intermittent breath-holds were performed by pausing the ventilator at end-expiration during MRI scans to minimize the effect of respiration.

During the course of the study protocol, an improved cine monitoring mode was developed with a "steady-state free precession" (SSFP) pulse sequence. 2D SSFP cine images were acquired continuously during the second 2-minute occlusion for the remaining 6 animals. The imaging parameters were 125-kHz BW; 128×256

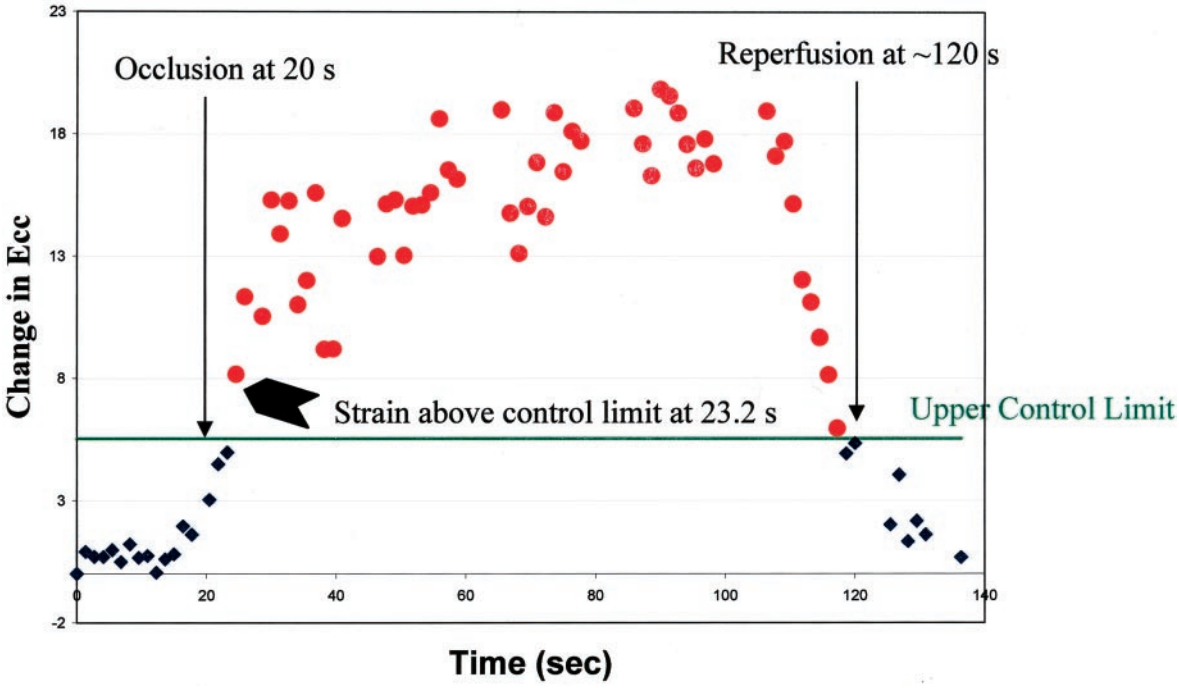

Figure 2. Control chart of user-independent quantitative FastHARP analysis of change in end-systolic circumferential strain (E_{cc}) versus time in ischemic regions of interest. Coronary artery occlusion occurred at 20 seconds (arrow), and strain values above upper control limit are shown in red circles, with first deviation occurring at 23.2 seconds (solid black chevron).

image matrix interpolated to 256×256; 28-cm FOV; number of excitations 0.5; 0.7-phase FOV; 3.9 ms TR; 1.9 ms TE; 45° flip angle; and 12 vps.

Data Analysis

The multi-coil raw k-space MRI data were reconstructed using a phase-sensitive procedure. Since a limited portion of k-space is acquired, tagged images were reconstructed using an alternative method. Using the magnitude image (**D**), representing the anatomy of the heart, and a harmonic phase image (**Φ**), indicating the motion of the myocardium, a synthetic tagged image is reconstructed by use of the formula $\mathbf{I}=\mathbf{D}+0.5\mathbf{D}\cos(2\mathbf{\Phi})+0.25\mathbf{D}\cos(4\mathbf{\Phi})+0.125\mathbf{D}\cos(6\mathbf{\Phi})$. By combining vertically and horizontally tagged images from alternating heartbeats, a synthetic grid tagged image is produced.

The 2D Eulerian circumferential strain was then calculated from the FastHARP image[11,12] and overlaid as a pseudocolor display on the synthetic tagged images by use of a MATLAB tool kit. Myocardial regions of abnormal contraction were identified in the HARP movies as regions with reductions in end-systolic circumferential strain relative to the preocclusion state. Two observers without knowledge of the location of the coronary occlusion bed determined and recorded, by consensus, the time after occlusion at which the reduction in end-systolic circumferential strain occurred, relative to the preocclusion state, on the FastHARP image.

The cine MRI images were displayed as continuously looping movies and were assessed for changes in wall thickening (ie, hypokinesis and akinesis) as evidence of WMA induced by coronary occlusion. The first cardiac phase during which WMAs were present was determined by a consensus of 2 observers.

To arrive at a semiquantitative assessment method rather than the visual consensus analysis of FastHARP, end-systolic circumferential strain (E_{cc}) was determined in 12 circumferential regions of interest with custom MATLAB-based software. Because the quantitative analysis software platform required transferring the FastHARP data to a personal computer for further analysis, the quantitative analysis was performed only in 4 representative studies in which the original magnitude and phase image data were retained. This observer-independent, semiquantitative assessment was performed offline after the completion of the animal studies. Curves of the change in end-systolic E_{cc} in the ischemic regions of interests versus time for each animal were analyzed with statistical control chart methods (NCSS Statistical Software) commonly used in quality control.[14] E_{cc} values before occlusion represented the expected variation in circumferential strain from heartbeat to heartbeat (ie, center line). These preocclusion values also allowed the calculation of upper and lower control limits. Values that fell outside the control limits (ie, out-of-control) could then be further investigated. In this particular study, the first out-of-control time point was considered to represent the onset of ischemia (Figure 2). This first ischemic time was subtracted from the time at which complete coronary artery occlusion occurred to determine an observer-independent prediction of the time of the onset of ischemia.

Postmortem Analysis

After formalin fixation, the excised heart rings were divided into transmural wedges (≈500 to 900 mg), which were subdivided into 3 transmural layers (ie, endocardial, midwall, and epicardial). These myocardial samples were weighed and counted in a γ-emission well spectrometer (model 5986, Hewlett Packard) along with the reference blood samples. Regional myocardial blood flow in the samples was calculated by standard techniques.[15] A myocardial sample with a 50% reduction in regional blood flow of the remote region by microspheres was defined as the ischemic region on coronary artery occlusion.

Statistical Analysis

Comparison of ischemia detection time between MRI techniques and ECG alterations was performed with a paired *t* test. All data were expressed as mean±SD, with a probability value of $P<0.05$ considered statistically significant.

Results

An LCx coronary occlusion was confirmed postmortem in 2 animals; the remaining 6 animals had LAD occlusion. On the basis of TTC staining, all animals had 100% viable myocar-

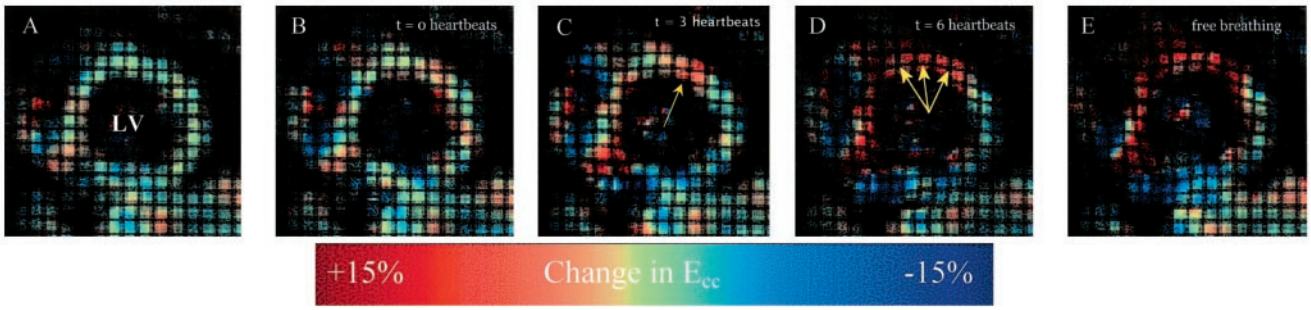

Figure 3. Representative end-systolic time frames of FastHARP acquisition with synthetic tags and a pseudocolor overlay of E_{cc} are shown in 1 animal. No change in strain is shown as green, decreased E_{cc} is shown as red (ie, decreased circumferential shortening or stretching), and increased E_{cc} is shown as blue (ie, increased circumferential shortening). Before coronary artery occlusion (A), uniform strain is present. After coronary artery occlusion (B), anterior wall shows decreased E_{cc} (ie, red area) at 3 heartbeats after occlusion (C). Area of dysfunction increases with time, concurrent with increased shortening in opposing wall (D, E). Pattern is still visible with free breathing (E). LV indicates left ventricle.

dium postmortem. In 2 animals, no region of ischemia was present with coronary artery occlusion, as assessed by microspheres. No area of WMA was detected on cine MRI or FastHARP imaging in these animals either.

Another animal suffered fatal arrhythmias before the third 2-minute coronary occlusion for injection of the radiolabeled microspheres. In this animal, the myocardial region distal to the coronary angioplasty balloon was confirmed by injection of Monastral blue dye into the coronary angioplasty catheter lumen. In the remaining 5 animals, microsphere analysis demonstrated severely reduced flow in the occluded coronary bed (0.031 ± 0.05 mL $\cdot g^{-1} \cdot min^{-1}$).

FastHARP Images

Images from representative synthetic tag time frames with an overlay of the FastHARP end-systolic circumferential strain are shown in Figure 3. In all studies, the pseudocolor map of circumferential strain was a fairly uniform green overlay on the synthetic tag images before coronary artery occlusion. A decrease in circumferential shortening or circumferential stretching was seen as a red color in the region of coronary artery occlusion. In 5 of 6 animals, there was an increase in circumferential shortening (seen as a blue area) in the opposite nonischemic myocardial wall. A graphic portrayal of the effects of free breathing on circumferential strain measurements is demonstrated in Figure 4.

Ischemia Detection

The onset of ischemia was detected significantly earlier by FastHARP than by cine MRI (9.5 ± 5 seconds FastHARP versus 33 ± 14 seconds cine, $P<0.01$). FastHARP ischemia detection preceded ECG changes, on average, by 54 seconds ($P<0.001$). The timing of ischemia detection by animal is given in the Table.

The Table also shows the onset of ischemia determined by the observer-independent control chart method applied to the change in systolic strain from FastHARP. Although this analysis was performed in only 4 animals, there was no significant difference in the time of ischemia detection by the visual method versus the observer-independent method ($P=0.5$). In 2 animals, an abrupt change in end-systolic E_{cc} resulted in almost identical timing of ischemia detection compared with the visual FastHARP method. In all animals, the ischemic time point was detected before cine MRI WMA.

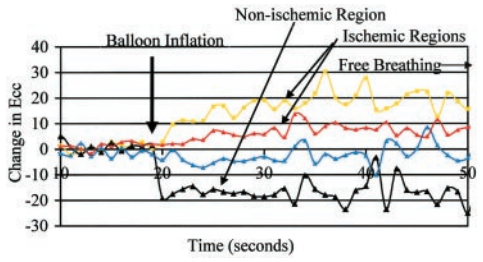

Figure 4. Change in end-systolic circumferential strain (E_{cc}) in 4 regions of interest from FastHARP image analysis shown for same animal as in Figure 3, demonstrating that ischemic regions can still be identified with free breathing.

Discussion

After coronary artery occlusion, a rapid sequence of events occurs, including changes in perfusion, function, and ECG as well as clinical manifestations, which has been called the "ischemic cascade."[16] Although perfusion abnormalities are generally thought to precede functional changes, which, in turn, occur before ECG changes or the development of chest pain, recent studies suggest that regional WMAs may occur almost simultaneously with perfusion abnormalities in cases of multivessel disease or at very high doses of dobutamine stress.[17]

Time of Ischemia Recognition After Coronary Occlusion by Technique in Animals With Demonstrated Ischemia

	FastHARP MRI			
Study	Visual	Semiquantitative	Cine MRI	ECG
1	6	...	25	90
2	6	...	30	90
3	10	6	60	38
4	17	18	24	75
5	15	21	31	45
6	3.2	3.2	28	43
Mean±SD	9.5±5	12±9	33±14*	63.5±24†

Values are in seconds.
*$P<0.01$ vs FastHARP visual MRI; †$P<0.003$ vs FastHARP visual MRI.

Other investigators have suggested that diastolic abnormalities precede systolic dysfunction and that these differences could be exploited with stress imaging techniques to increase the sensitivity of detecting myocardial ischemia. However, studies performed in both pigs and dogs have shown that systolic and diastolic dysfunction often occur almost simultaneously or that systolic dysfunction actually precedes diastolic dysfunction.[18–20] In an attempt to resolve the controversy, Mor-Avi et al[20] demonstrated that the order of diastolic and systolic dysfunction from coronary ischemia could be determined by use of color-coded images of endocardial motion from echocardiographic images as a diagnostic aid in detecting stress-induced WMA. In this swine study of acute ischemia, systolic dysfunction preceded diastolic dysfunction with nearly equal frequency. However, this study demonstrated the benefit of a color-coded display as an objective method of tracking wall-motion changes.

Our study demonstrated the ability of FastHARP MRI to monitor the ischemic cascade in real time and to detect quantitatively the onset of ischemia in a model of acute coronary occlusion. In 6 of 8 animals, we were able to detect ischemia by both cine and FastHARP MRI. The onset of ischemia as characterized by these 2 methods was in agreement with the demonstrated territory of acute occlusion based on radioactive microspheres or blue dye staining. In the remaining 2 animals, neither MRI method nor microsphere evaluation of blood flow demonstrated an ischemic region. Thus, despite the small number of animals studied, a highly significant improvement in the time to detection of ischemia was demonstrated with FastHARP MRI without the introduction of false-positives.

Our results demonstrate that FastHARP MRI can be used to detect ischemia considerably earlier than 2 commonly used cine MRI techniques, as well as ECG changes after acute coronary occlusion. The earlier detection of ischemia by FastHARP most likely reflects the improved ability to resolve changes in regional strain rather than transmural thickening. Ischemic alterations are known to occur earlier in subendocardial than in subepicardial layers. However, significant reductions in transmural wall thickening probably require reductions in both the subendocardial and subepicardial layers. Thus, FastHARP MRI is capable of detecting alterations in regional shortening that precede the reduction of transmural thickening.

Moreover, because FastHARP MRI can be rapidly analyzed to display a pseudocolor map of strain overlaid on synthetic tag images, the level of observer training to detect ischemia is markedly diminished relative to cine WMA detection. In addition, the control chart technique is amenable to implementation as a real-time monitoring technique using updated values of E_{cc} for each heartbeat, as might occur in a cardiac stress test.

This earlier detection of induced ischemia by FastHARP MRI could be used to terminate a stress test before the development of adverse signs (eg, arrhythmias, hemodynamic problems, etc) or to treat these symptoms more rapidly. In addition, the use of a color display may improve the visualization of WMAs. Moreover, the semiquantitative evaluation of the change in end-systolic circumferential strain determined from FastHARP MRI in these studies demonstrates that ischemia detection could potentially be performed in a totally nonsubjective manner. Future studies with multiple readers will be needed to assess the impact of using more objective criteria for the detection of ischemia and thus better standardization and less operator dependence in cardiac stress testing.

Limitations

Because most preconditioning models use more than four 5-minute ischemic episodes, ischemic preconditioning was probably not induced in the present study. Despite MRI not being randomized, ECG alterations were not different on the second occlusion, nor were WMAs present between ischemic episodes. However, because microsphere blood-flow validation of ischemia was performed after MRI, the ischemic severity may not be identical during all occlusions.

A trend toward more rapid ischemia detection by cine MRI relative to ECG ischemic changes was observed ($P<0.08$). However, these cine data are from 2 similar but distinct cine MRI techniques in a limited number of studies. Thus, additional studies could increase the statistical power and may demonstrate a significant difference between cine MRI and ECG changes. Despite the small number of animals, a highly statistically significant improvement in the time of ischemia detection with FastHARP MRI relative to the cine MRI and ECG changes was demonstrated, with a statistical power of 0.90 and 0.95, respectively. Therefore, the FastHARP technique, which demonstrates quantitative wall motion information, with slightly more than a heartbeat delay including image reconstruction and analysis time, shows enormous potential for the real-time, online rapid detection of ischemia viewed as WMAs.

Conclusions

In conclusion, in the present study, we have developed a new method for rapid acquisition and detection of strain alterations using FastHARP MRI that allows earlier detection of ischemia. In addition, the method allows rapid operator-independent monitoring of regional contractility in quantitative terms. Therefore, FastHARP MRI shows promise, because of speed of imaging and analysis, for use during MR stress testing.

Acknowledgments

This work was supported by grants RO1-HL47405, RO1-HL63439, RO1-HL45090, and KO2-HL04193 from the National Institutes of Health National Heart, Lung, and Blood Institute and from the Fundación Ramón Areces, Madrid, Spain.

References

1. Poldermans D, Fioretti PM, Boersma E, et al. Long-term prognostic value of dobutamine-atropine stress echocardiography in 1737 patients with known or suspected coronary artery disease: a single-center experience. *Circulation*. 1999;99:757–762.
2. Grover-McKay M, Matsuzaki M, Ross JJ. Dissociation between regional myocardial dysfunction and subendocardial ST segment elevation during and after exercise-induced ischemia in dogs. *J Am Coll Cardiol*. 1987; 10:1105–1112.
3. Nagel E, Lehmkuhl H, Bocksch W, et al. Noninvasive diagnosis of ischemia-induced wall motion abnormalities with the use of high-dose dobutamine stress MRI: comparison with dobutamine stress echocardiography. *Circulation*. 1999;99:763–770.

4. Hundley WG, Hamilton CA, Thomas MS, et al. Utility of fast cine magnetic resonance imaging and display for the detection of myocardial ischemia in patients not well suited for second harmonic stress echocardiography. *Circulation*. 1999;100:1697–1702.
5. Al-Saadi N, Nagel E, Gross M, et al. Noninvasive detection of myocardial ischemia from perfusion reserve based on cardiovascular magnetic resonance. *Circulation*. 2000;101:1379–1383.
6. Chia JM, Fischer SE, Wickline SA, et al. Performance of QRS detection for cardiac magnetic resonance imaging with a novel vectorcardiographic triggering method. *J Magn Reson Imaging*. 2000;12:678–688.
7. Pohost GM, Biederman RW. The role of cardiac MRI stress testing: "Make a better mouse trap. . .." *Circulation*. 1999;100:1676–1679.
8. Axel L, Dougherty L. Heart wall motion: improved method of spatial modulation of magnetization for MR imaging. *Radiology*. 1989;172:349–350.
9. Zerhouni EA, Parish DM, Rogers WJ, et al. Human heart: tagging with MR imaging: a method for noninvasive assessment of myocardial motion. *Radiology*. 1988;169:59–63.
10. Gotte MJ, van Rossum AC, Twisk JWR, et al. Quantification of regional contractile function after infarction: strain analysis superior to wall thickening analysis in discriminating infarct from remote myocardium. *J Am Coll Cardiol*. 2001;37:808–817.
11. Osman NF, Kerwin WS, McVeigh ER, et al. Cardiac motion tracking using CINE harmonic phase (HARP) magnetic resonance imaging. *Magn Reson Med*. 1999;42:1048–1060.
12. Osman NF, McVeigh ER, Prince JL. Imaging heart motion using harmonic phase MRI. *IEEE Trans Med Imaging*. 2000;19:186–202.
13. Axel L, Dougherty L. MR imaging of motion with spatial modulation of magnetization. *Radiology*. 1989;171:841–845.
14. Davies OL. *Statistical Methods in Research and Production*. London, UK: Oliver and Boyd; 1961.
15. Domenach RV, Hoffman JIE, Noble MIM, et al. Total and regional coronary blood flow measured by radioactive microspheres in conscious and anesthetized dogs. *Circ Res*. 1969;21:581–596.
16. Nesto RW, Kowalchuk GJ. The ischemic cascade: temporal sequence of hemodynamic, electrocardiographic and symptomatic expressions of ischemia. *Am J Cardiol*. 1987;59:23C–30C.
17. Leong-Poi H, Rim SJ, Le DE, et al. Perfusion versus function: the ischemic cascade in demand ischemia: implications of single-vessel versus multivessel stenosis. *Circulation*. 2002;105:987–992.
18. Ihara T, Komamura K, Shen YT, et al. Left ventricular systolic dysfunction precedes diastolic dysfunction during myocardial ischemia in conscious dogs. *Am J Physiol*. 1994;267:H333–H343.
19. Derumeaux G, Ovize M, Loufoua J, et al. Doppler tissue imaging quantitates regional wall motion during myocardial ischemia and reperfusion. *Circulation*. 1998;97:1970–1977.
20. Mor-Avi V, Collins KA, Korcarz CE, et al. Detection of regional temporal abnormalities in left ventricular function during acute myocardial ischemia. *Am J Physiol*. 2001;280:H1770–H1781.